EUMETSAT OSI SAF
OCEAN AND SEA ICE

ASCAT-C wind product calibration and validation

Global OSI SAF 25 km wind product (OSI-102-c)

Global OSI SAF coastal wind product (OSI-104-c)

Regional EARS 25 km and coastal wind products

Version: 1.3

Date: 27/11/2019

Jeroen Verspeek, Anton Verhoef, and Ad Stoffelen

Royal Netherlands
Meteorological Institute
Ministry of Infrastructure
and Water Management

Document Change record

Document version	Software version	Date	Author	Change description
1.0		19/4/2019	JV, AS	First version and revision
1.1		3/6/2019	AV	Applied OSI SAF template, added buoy and triple collocation validations, EARS product validation
1.2		12/9/2019	AV	Some changes resulting from Operational Readiness Review RIDs.
1.3		27/11/2019	JV	Included Cone Metrics results

Table of contents

1. Introduction

The EUMETSAT Ocean and Sea Ice Satellite Application Facility (OSI SAF) produces a range of air-sea interface products, namely: wind, sea ice characteristics, Sea Surface Temperatures (SST) and radiative fluxes, Surface Solar Irradiance (SSI) and Downward Long wave Irradiance (DLI). The Product Requirements Document [1] provides an overview of the committed products and their characteristics in the current OSI SAF project phase, the Service Specification Document [2] provides specifications and detailed information on the services committed towards the users by the OSI SAF in a given stage of the project.

The Advanced SCATterometer (ASCAT) is one of the instruments carried on-board the Meteorological Operational (Metop) polar satellites launched by the European Space Agency (ESA) and operated by the EUropean organisation for the exploitation of METeorological SATellites (EUMETSAT). Metop-A, the first in a series of three satellites, was launched on 19 October 2006, Metop-B was launched on 17 September 2012 and Metop-C was launched on 7 November 2018.

The OSI SAF delivers operational level 2 wind products with 25 and 12.5 km Wind Vector Cell (WVC) spacing in near-real time [3], based on the ASCAT level 1b products. See the EUMETSAT documentation [4], [5] for more information on the level 1b product characteristics. The 12.5 km products (also referred to as 'coastal products') use the so-called box-car spatial filtering, contrary to the 25 km products which use a Hamming spatial filtering [3].

Within the framework of the OSI SAF, KNMI has developed an ocean calibration method, based on Numerical Weather Prediction (NWP) wind inputs, the so-called NWP Ocean Calibration (NOC). The NOC method [6], [7] improves the consistency of the backscatter distributions measured by the six ASCAT radar beams at each incidence angle and therefore improves geophysical retrievals that combine the radar beam measurements. The NOC method has the advantage over other calibration methods (e.g., transponders, rain forest, ice) that it can be applied over a large global area (all the oceans) that provides a substantial amount of data and thus more accurate results over a relatively short period of time. It is therefore also very suitable for monitoring purposes. In this report, NOC corrections are derived from and subsequently applied to ASCAT-C data. Then the resulting level 2 products are analysed.

In section 2 the NWP ocean calibration method is explained and the derivation of the NOC corrections for ASCAT-C is described. Section 3 shows how the NOC corrections help to improve the wind retrieval results. In the rest of this report, we assess the quality of the new OSI SAF wind products based on Metop-C and we will mainly focus on the differences between Metop-C and Metop-A/B products. We compare the scatterometer wind data with ECMWF model data in section 4 and with in situ wind data from moored buoys in section 5. Section 6 shows the results from a triple collocation study using winds from the scatterometer, buoys, and ECMWF together. In section 7 the regional EARS winds from Metop-C are compared with the global OSI SAF winds. Section 8 summarises the main conclusions.

1.1. Acknowledgement

We are grateful to Jean Bidlot of ECMWF for helping us with the buoy data retrieval and quality control. Jur Vogelzang of KNMI helped to obtain the triple collocation results.

2. NWP Ocean Calibration

2.1. NOC method

The Numerical Weather Prediction Ocean Calibration (NOC) technique [7] is used to assess the difference between scatterometer backscatter data, and simulated backscatter data out of collocated NWP winds using the GMF. Discrepancies between mean measured and simulated backscatter may be due to instrument calibration, systematic and random errors in NWP wind speed and direction, and GMF errors. These sources of error should therefore be analysed carefully. The NOC method is based on the analysis of a large measurement dataset to estimate Fourier coefficients that can be directly compared to those in the CMOD7 GMF. For any particular WVC in any beam the incidence angle is virtually constant around the orbit and we can model the backscatter with

$$\sigma_0(V,\phi) = B_0(V)[1+B_1(V)+B_2(V)\cos(2\phi)]^{1.6}$$

where V is wind speed and Φ is the wind direction with respect to the beam pointing direction. The mean backscatter is essentially determined by the value of B_0 with contributions from B_1 and B_2. In z-space, where $z = \sigma_0^{0.625}$, this becomes

$$z(V,\phi) = \frac{1}{2}a_0(V)+a_1(V)\cos(\phi)+a_2(V)\cos(2\phi)$$

where $a_0 = 2B_0^{0.625}$, $a_1 = B_1B_0^{0.625}$ and $a_2 = B_2B_0^{0.625}$. Integrating uniformly over azimuth angle gives

$$\frac{1}{2\pi}\int_0^{2\pi} z(V,\phi)d\phi = \frac{1}{2}a_0(V)$$

So, when the wind direction distribution is sampled uniformly for all wind speeds, then the mean of $2a_0$ should be identical to the mean of z. This means that uncertainties in a_1 and a_2 do not contribute to the error in the simulated mean z.

To arrange for a uniform wind direction distribution at each wind speed, we split the data into wind speed bins and azimuth angle bins. Bins are defined such that they are large enough to contain a certain minimum number of measurements and small enough to provide a good approximation of the integral. In the following, indices i and j refer to wind speed bin i and azimuth angle bin j respectively. Index k is used to refer to an individual measurement z_k. Parameters I, J and K refer to the total number of bins or measurements, so $i = 1, 2 ..., I$, $j = 1, 2 ... , J$ and $k = 1, 2 ... , K(i,j)$.

The mean z in a fixed wind speed row is, lets call this $z(i)$:

$$z(i) = \frac{1}{J}\sum_{j=1}^{J}\frac{1}{K(i,j)}\sum_{k=1}^{K(i,j)} z_k(i,j)$$

Summation over the wind speed rows gives

$$\langle z\rangle = \frac{1}{KJI}\sum_{i=1}^{I} KJ(i)z(i)$$

with

$$KJ(i) = \sum_{j=1}^{J} K(i,j), \qquad KJI = \sum_{i=1}^{I} KJ(i)$$

<z> is the mean backscatter value over all speeds at a uniform wind direction distribution and may be either measured or simulated by collocated NWP wind inputs and the GMF, where mainly the term as given by $a_0(V)$ or $B_0(V)$ contributes. Any discrepancy between the simulated and measured mean backscatter values is computed as a ratio. A ratio not equal to one may be related to inaccuracies in the instrument gain, e.g., beam pattern determination, or to errors in the NWP input winds and GMF. Here, we use the NOC to correct for instrument gain in order to obtain consistency of the backscatter distributions measured by the six ASCAT radar beams at each incidence angle and validate its effects.

The NWP and GMF related errors slightly decrease with enhanced sampling over all seasons and are estimated to be within 0.1 dB for a one-year calibration period [6], [7]. This method needs only a few days of collocated ASCAT data and ECMWF winds to produce a reasonable estimate of difference in a_0 within 0.2 dB. We use CMOD7 [8] with ECMWF stress-equivalent 10-meter winds [9] to calculate collocated model backscatter values corresponding to the measured values and apply the process as described above. The ratio of the two values of a_0 then provides an estimate of the mean difference between model and measurement backscatter, i.e., instrument antenna gain.

2.2. ASCAT-C ocean calibration residuals

The ocean calibration is performed on ASCAT-C data over a period of one month from 2019-02-26 to 2019-03-26 for both the coastal (12.5 km WVC spacing with box filtering) and the 25 km product (with Hamming window spatial filtering). The data is quality controlled and a conservative lat-lon filter is applied in order to rule out possible sea-ice contamination. The resulting pattern in shown in Figure 1.

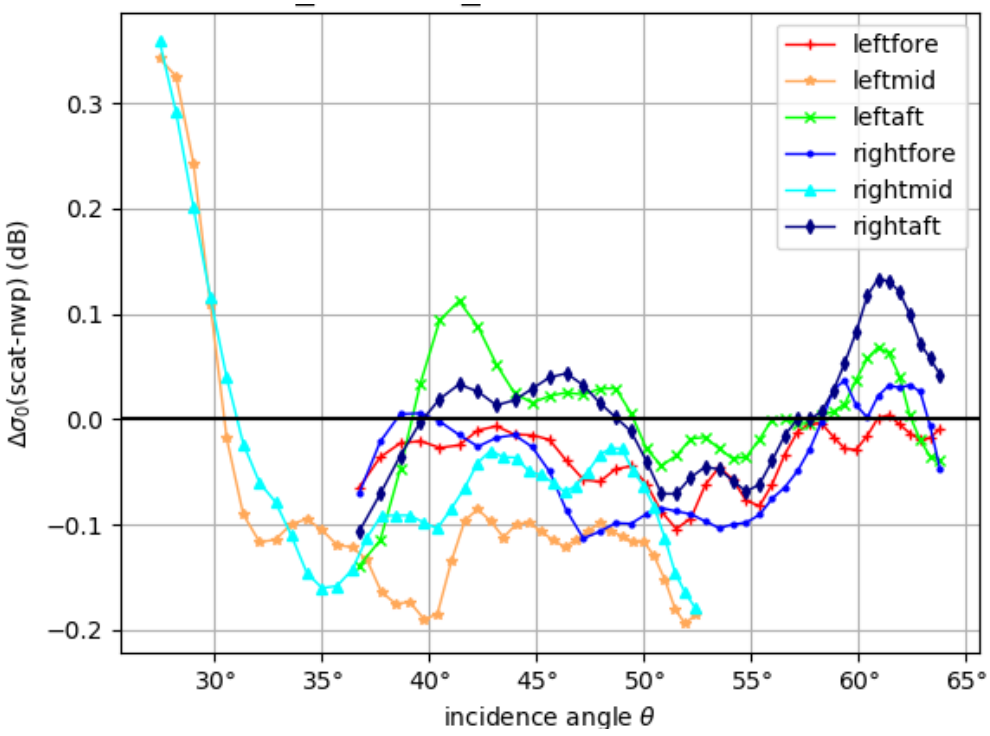

Figure 1: Average of the NWP ocean calibration residuals of ASCAT-C over the period 2019-02-26 to 2019-03-26 for the coastal product, using ECMWF stress-equivalent 10-m winds and CMOD7 as GMF.

The figure shows residuals in the range from about +0.3 dB to -0.2 dB. At low incidence angle the residuals are the largest, but still significantly smaller with the use of the improved GMF CMOD7 instead of the previous version CMOD5.n (not shown). Similar patterns are observed for ASCAT-B and ASCAT-A. Also wiggles in each of the antenna residuals are present, similar to those of ASCAT-B and ASCAT-A, see Figure 2. The residuals as shown are used as backscatter correction factors in the ASCAT Wind Data Processor (AWDP).

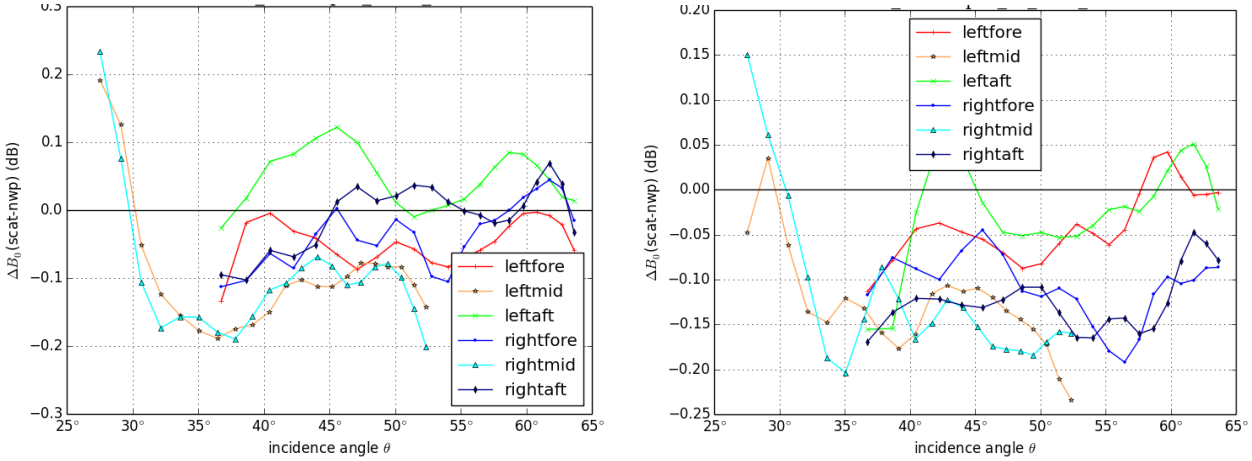

Figure 2: Average of the NWP ocean calibration residuals of ASCAT-A (left) and ASCAT-B (right) over 2013, using ECMWF stress-equivalent 10-m winds and CMOD7 as GMF.

Note that the ASCAT-C backscatter data used in this report have not yet been calibrated using ground transponders; a calibration campaign is done during the first half of 2020. Based on the results of the campaign, a calibration update for ASCAT-C is expected to take place late 2020. From Figure 1 and Figure 2 it is clear that the ASCAT-C calibration is already close to the ASCAT-A and ASCAT-B calibrations, so only a small change of backscatter values is expected. To minimise the impact on wind calibration, OSI SAF will cooperate with EUMETSAT and parallel level 1 data sets will be made using the old and new calibrations. The differences will be used to re-compute the backscatter corrections in the wind processor. In this way, a smooth transition for the wind users is guaranteed.

3. Effect of NOC on wind retrievals

3.1. Measurement space visualisation

The radar backscatter triplets can be visualized in a 3-dimensional measurement space. For a given Wind Vector Cell (WVC), i.e., position across the swath, the measured triplets are distributed around the GMF, which constitutes a well-defined conical surface that depends on wind speed and wind direction only [10]. Systematic displacements of the cloud of triplets in any direction of the 3D space are mainly due to absolute beam biases, which are adequately removed by the results of the NOC [6], hence beneficially affecting the ASCAT geophysical retrievals.

Visualisations of the data triplets in measurement space together with the CMOD7 GMF have been made in order to see how well the GMF fits the cloud of measurements. The (fore, mid, aft) triplets are transformed to (*x, y, z*)-coordinates:

$$x = \frac{\sigma^0_{\text{fore}} + \sigma^0_{\text{aft}}}{\sqrt{2}}$$

$$y = \frac{\sigma^0_{\text{fore}} - \sigma^0_{\text{aft}}}{\sqrt{2}}$$

$$z = \sigma^0_{\text{mid}}$$

Figure 3 shows the cone intersection with the plane $x = C$, where the constant C corresponds to a wind speed V = 8 m/s at $\Phi = 0$ (upwind). Data triplets within a distance of $0.001C$ of the plane are shown. NOC corrections are applied in the left plot and not in the right plot.

Figure 4 shows the cone intersection with the plane $y = 0$. Data triplets within a distance of $0.001x$ of the plane are also shown. Although there are differences, the figures show a good fit on the eye, both with and without NOC corrections. The Cone Metrics method [11] is comparing measurement clouds in an automated iterative process and is capable of finding an optimal shift between the two clouds.

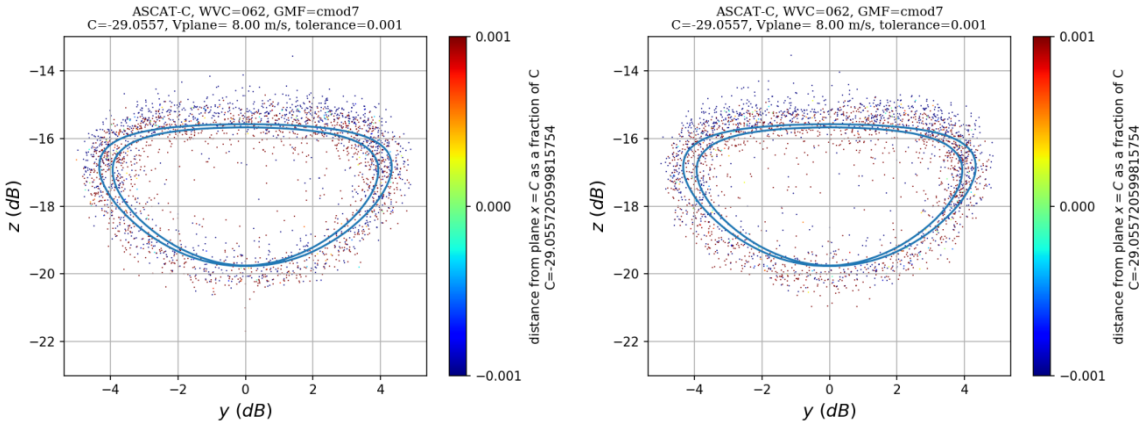

Figure 3: Visualisation of CMOD7 for WVC 62 (coastal product, right swath, incidence angle fore/aft = 52.9°, mid = 41.7°) together with data triplets. Intersection of the cone with the plane x = C. The value of C corresponds to a wind speed of v = 8.0 m/s at $\phi = 0$. Triplets within a distance of $\pm 0.001C$ from the mentioned plane are plotted. Data is from March 2019 with NOC corrections applied on the left plot, without NOC corrections on the right plot.

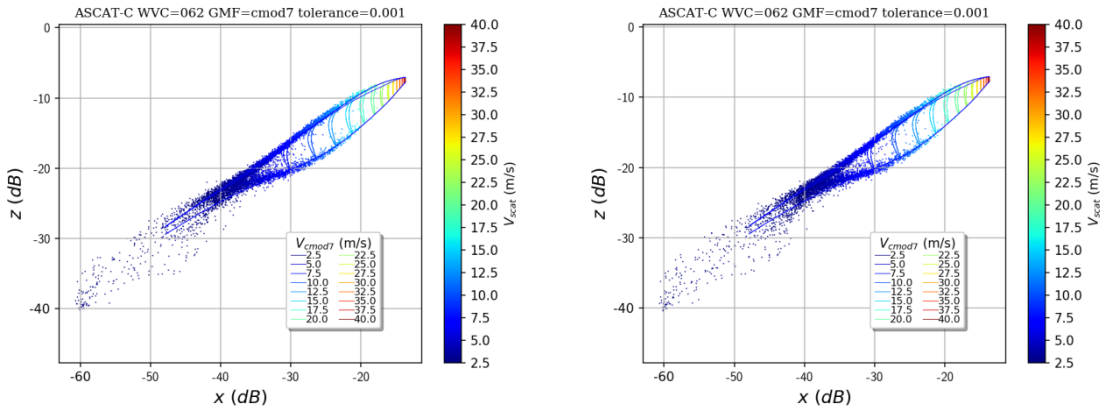

Figure 4: Visualisation of CMOD7 for WVC 62 (coastal product, right swath, incidence angle fore/aft = 52.9°, mid = 41.7°) together with data triplets. Intersection of the cone with the plane y = 0. Triplets within a certain distance (0.001x) from the mentioned plane are plotted. Data is from March 2019 with NOC corrections applied on the left plot, without NOC corrections on the right plot.

3.2. Cone Metrics

Cone metrics (CM) is a method to calibrate scatterometers. Traditional calibration methods involve comparison to a geophysical phenomenon like ocean winds, rain forest backscatter or ice. These traditional methods require that the geophysical phenomenon is either constant (e.g. ice), has a well-known behaviour in time, or has a well-known averaged value (ocean winds). Also, they require a GMF in order to translate the geophysical parameters to a backscatter value. Cone metrics compares to backscatter values from a scatterometer and tries to avoid influence as much as possible from other geophysical phenomena and the GMF. Thus their uncertainties are minimized.

A reference to compare to could be either a past period from the same scatterometer or a comparable scatterometer. It can be used for intercalibration of two scatterometers, e.g., a recently launched scatterometer and an existing scatterometer of the same type. It can also be used for trend monitoring by comparing recent data from a scatterometer to data from a stable reference period [11].

In Figure 5 the CM residuals (left) and NOC double difference residuals (right) are shown from ASCAT-C March 2019 data with ASCAT-B data from 2013 as reference. The NOC double difference is simply computed as the difference between two NOC residuals, in this case the ASCAT-B 2013 NOC residuals are subtracted from the ASCAT-C March 2019 residuals. In the NOC double difference the effects of NWP wind speed Probability Density Function and GMF errors are mostly cancelled out. In CM these effects play no role whatsoever since they are not used.

The trends as a function of incidence angle per antenna are comparable for the two methods, the wiggles are reproduced with a high accuracy in the order of ~0.01 dB. There is an overall offset of ~0.1 dB and a smaller additional offset per antenna.

In Figure 6 the trend in CM residuals (left) and NOC residuals (right) is shown for ASCAT-C for each month from March to August 2019. Here the residuals are averaged over the incidence angles or WVCs to yield a single value per antenna. Both methods give stable residuals per antenna to within ~0.05 dB for this period. The NOC residuals seem to have a more upward trend over time than the CM residuals. NOC is known to have a seasonal effect due to dependency on the NWP wind speed Probability Density

Function. This seasonal effect is not present in CM and could be an explanation for the difference in trends from CM and NOC.

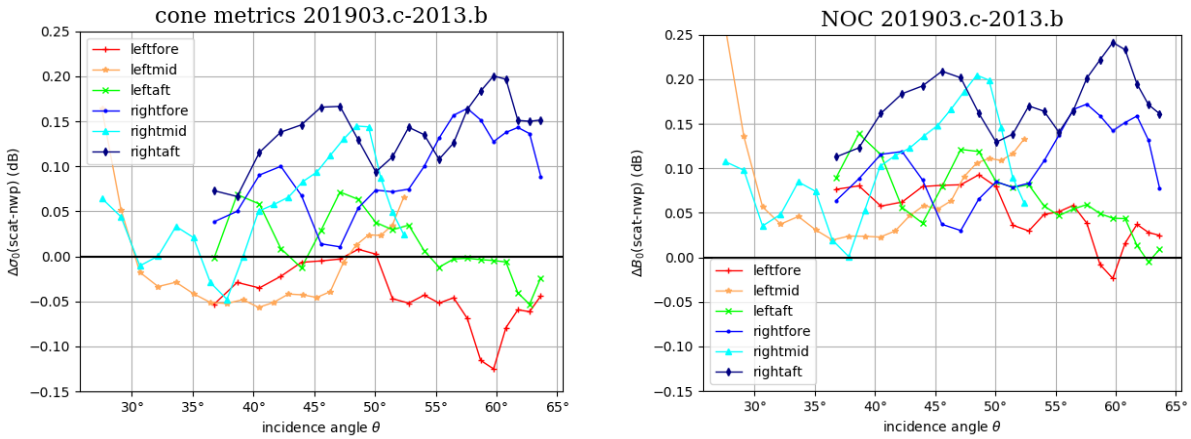

Figure 5: Cone Metrics residuals (left) and corresponding NOC double difference residuals (right) from ASCAT-C March 2019 data compared to ASCAT-B 2013 data.

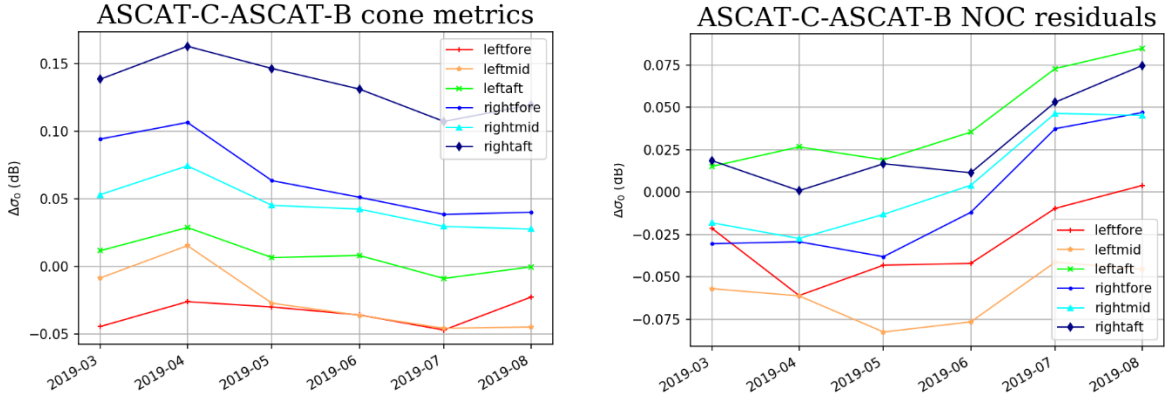

Figure 6: Residuals from Cone Metrics analysis (left) and NOC analysis (right) for each month from March to August 2019 of ASCAT-C The reference is ASCAT-B 2013 data in both cases.

Both figures confirm the high relative and absolute accuracy of both methods and their ability to detect and study instrumental anomalies. This result also confirms the stability of ASCAT-C and gives a good calibration relative to ASCAT-B and thus also to ASCAT-A.

3.3. Effect on MLE values

The Maximum Likelihood Estimator (MLE) is the normalised distance in 3D measurement space from a measurement triplet to the point on the wind cone that corresponds to the retrieved wind. It is a measure of how well the measurements and GMF fit to each other. The MLE is normalised using a table in order to get an expectation value of <|MLE|> = 1 for each WVC (<|MLE|> denotes the average of the absolute value of the MLE). The MLE normalisation table is the same for all ASCAT scatterometers.

Figure 7 shows the average of the |MLE| and MLE value per WVC for ASCAT-C coastal winds. The green lines are with NOC corrections applied, the blue lines is the same without the correction. Especially for

the innermost WVCs the positive impact of NOC is large. Figures for ASCAT-A and ASCAT-B are similar (not shown here).

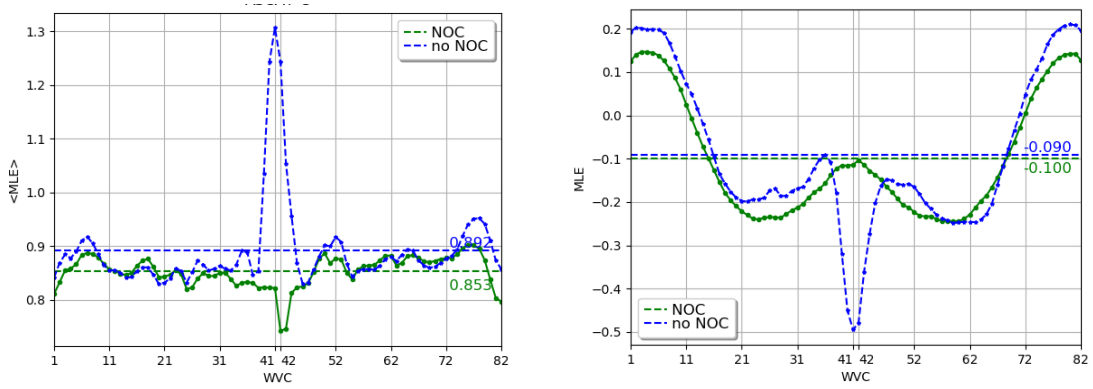

Figure 7 - Value of <|MLE|> on the left and <MLE> on the right. The green plots have NOC corrections applied. 12.5 km WVC spacing data is used from March 2019.

3.4. Effect on Quality Control

The occurrence ratio of some relevant level 2 Quality Control (QC) flags and their WVC dependency is shown in Figure 8 for ASCAT-C. The GMF distance flag is set when the measured triplet has an anomalously large distance to the GMF cone, while the Variational QC flag is set during 2DVAR ambiguity removal when a wind vector is spatially inconsistent with its neighbours. The KNMI QC flag which is shown in the figure is based on the GMF distance flag in sea ice-free regions. The solid lines are obtained with NOC corrections applied. The dashed lines in the left plot are without NOC corrections. In the plot on the right the dashed lines are not visible on this scale. For the innermost WVCs the NOC corrections have a large positive effect on the Variational QC flagging, the rejection rate is largely reduced. All fractions are low (except for high winds) and comparable to ASCAT-B and ASCAT-A.

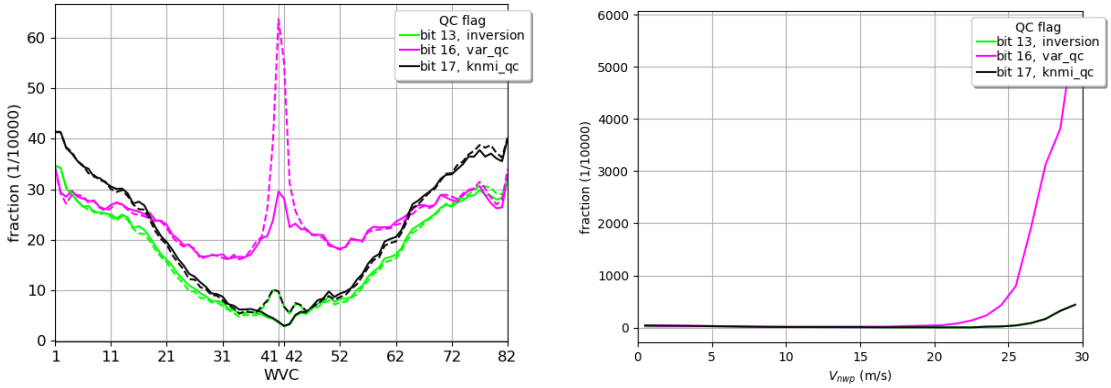

Figure 8: Some level 2 quality flag occurrence ratios as a function of WVC (left) and as a function of wind speed (right). The solid lines are with NOC corrections applied, the dashed lines are without NOC corrections. March 2019 ASCAT-C coastal data is used.

The rejection rate increases when we go from the inner part to the outer part of the swath. This can be explained as follows. The GMF cone opens up with incidence angle. Therefore, larger MLE values inside the cone are more frequent in the outer swath (less aliasing effect). Also noise is somewhat lower at higher incidence angles, which reduces the MLE norm. These effects bring more data into the tail of the MLE distribution at high incidence angles and therefore increase the QC rejection rate.

In Table 1 the KNMI QC and VAR QC rejection rates are compared for the three ASCAT instruments. They are very much alike.

	Total	KNMI QC	Fraction KNMI QC	VAR QC	Fraction VAR QC
12.5 km Metop-A	52,159,534	104,411	0.200%	120,309	0.231%
12.5 km Metop-B	52,161,552	107,876	0.207%	122,079	0.234%
12.5 km Metop-C	51,169,029	105,696	0.207%	120,109	0.235%

Table 1: Comparison of KNMI QC and Variational QC rejection rates for the ASCAT scatterometers. March 2019 coastal data is used.

4. Comparison with NWP model wind data

Figure 9 shows two-dimensional histograms of the retrieved winds versus background ECMWF stress-equivalent 10 m winds for the Metop-C 25 km wind product, after rejection of Quality Controlled (KNMI QC flagged) wind vectors. The data for these plots are from 42 consecutive orbits from 1 to 3 April 2019. Due to the large daily number of collocations with the model data, three days is sufficient to obtain reliable statistics. The seasonal oscillations are also known to be quite small for these type of comparisons. The top left plot corresponds to wind speed (bins of 0.5 m/s) and the top right plot to wind direction (bins of 2.5°). The latter are computed only for ECMWF winds larger than 4 m/s. The bottom contour plots show the zonal (*u)* and meridional (*v)* wind component statistics (bins of 0.5 m/s). The contour lines are in logarithmic scale.

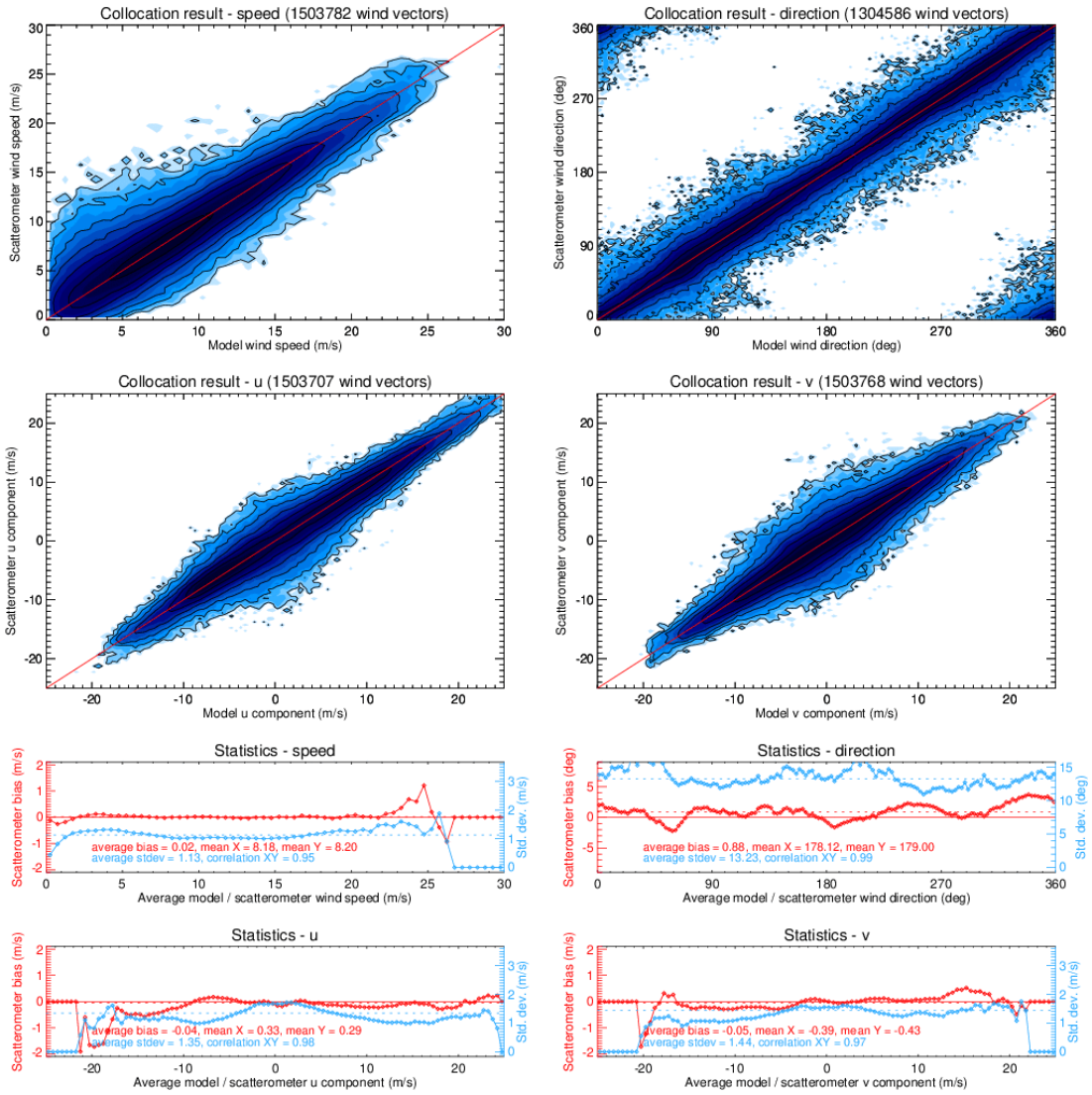

Figure 9: Two-dimensional histograms of wind speed, direction (w.r.t. wind coming from the North), u and v components of 25 km ASCAT-C wind product versus the ECMWF model forecast winds (stress-equivalent 10m winds) from 1-3 April 2019 (top panels). The corresponding biases (red) and standard deviations (blue) as a function of the average scatterometer and model winds are shown in the bottom.

Figure 10 shows the same comparison for 12.5 km Metop-C winds of 1 April 2019 (14 consecutive orbits). Only one day of data is sufficient now to obtain a large number of colocations. Both the 25 km and 12.5 km results look very much the same as those from Metop-A and Metop-B, which are not shown here but summarised in Table 2. It is clear that all three instruments show comparable statistics when compared to ECMWF winds when looking at the 25 km and 12.5 km products.

The 25 km ASCAT wind components compare slightly better to ECMWF than the 12.5 km ASCAT wind components, as can be seen in Table 2. This is in line with the relatively coarse effective resolution of the ECMWF model data [15]; the NWP winds better resemble the lower resolution 25 km winds than the 12.5 km winds. The ASCAT wind speed biases and wind component standard deviations are all well within the OSI SAF requirements: better than 2 m/s in wind component standard deviation with a bias of less than 0.5 m/s in wind speed.

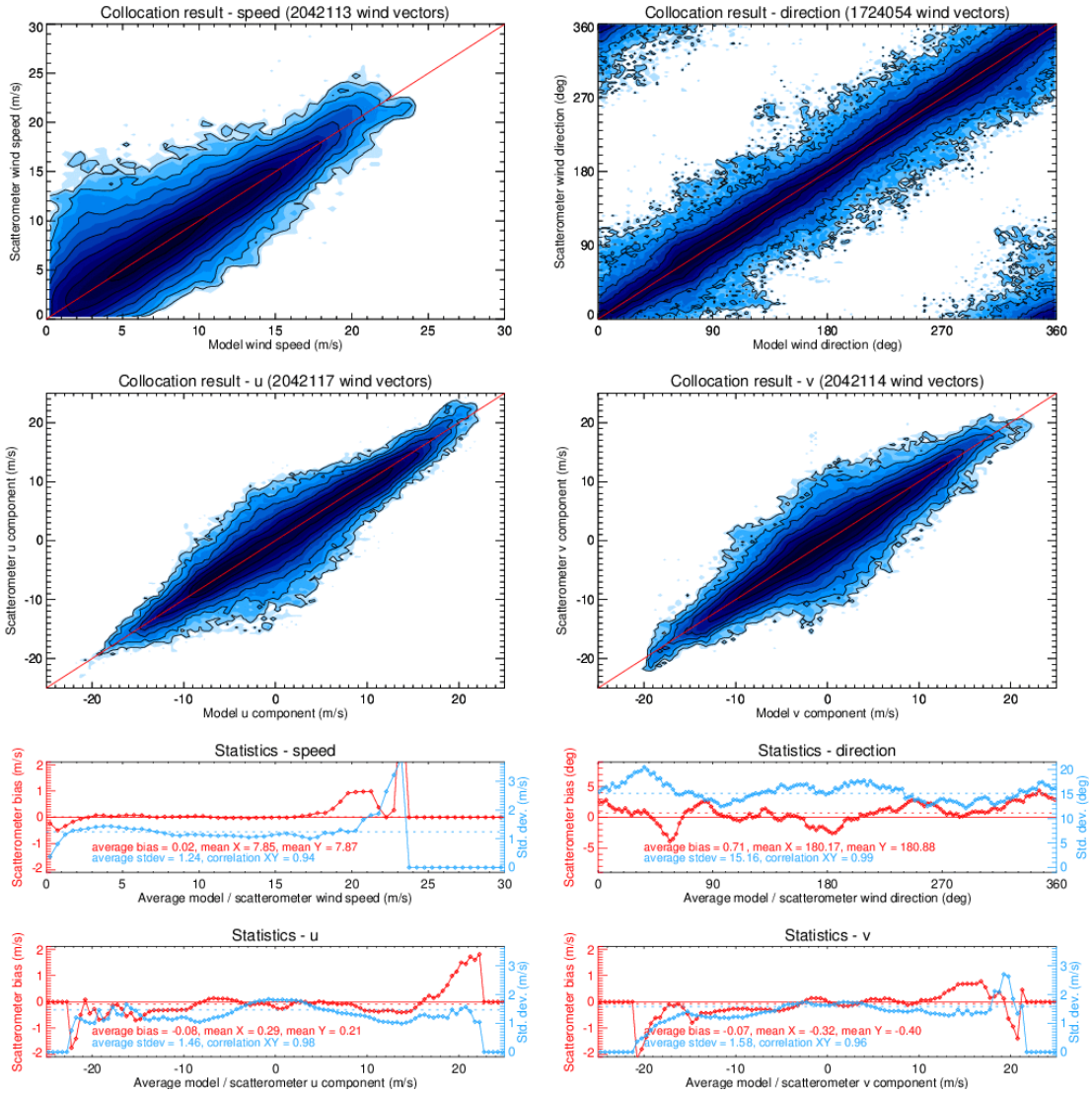

Figure 10: Two-dimensional histograms of wind speed, direction (w.r.t. wind coming from the North), u and v components of 12.5 km ASCAT-C wind product versus the ECMWF model forecast winds (stress-equivalent 10m winds) from 1 April 2019 (top panels). The corresponding biases (red) and standard deviations (blue) as a function of the average scatterometer and model winds are shown in the bottom.

	# of wind vectors	speed bias	stdev *u*	stdev *v*
25 km Metop-A	1,538,083	0.10	1.36	1.42
25 km Metop-B	1,537,049	0.05	1.37	1.42
25 km Metop-C	**1,503,707**	**0.02**	**1.35**	**1.44**
12.5 km Metop-A	2,087,439	0.03	1.48	1.60
12.5 km Metop-B	2,093,484	0.04	1.47	1.57
12.5 km Metop-C	**2,042,117**	**0.02**	**1.46**	**1.58**

Table 2: ECMWF comparison results of ASCAT 25 km and 12.5 km wind products.

5. Buoy validations

In this section, scatterometer wind data are compared with in situ buoy wind measurements. The buoy winds are distributed through the Global Telecommunication System (GTS) and have been retrieved from the ECMWF MARS archive. The buoy data are quality controlled and (if necessary) blacklisted by ECMWF [12]. We used a set of 94 moored buoys spread over the oceans, most of them in the tropical oceans and near Europe and North America. These buoys are also used in the validations that are routinely performed for the OSI SAF wind products; see the links on http://www.knmi.nl/scatterometer/osisaf/. The buoy winds are measured hourly by averaging the wind speed and direction over 10 minutes. The real winds at a given anemometer height have been converted to 10-m equivalent neutral winds using the Liu, Katsaros and Businger (LKB) model [12], [13] in order to enable a good comparison with the 10-m scatterometer winds.

See Figure 11 for the locations of the buoys used in the comparisons. A scatterometer wind and a buoy wind measurement are considered to be collocated if the distance between the WVC centre and the buoy location is less than the WVC spacing divided by √2 and if the acquisition time difference is less than 30 minutes.

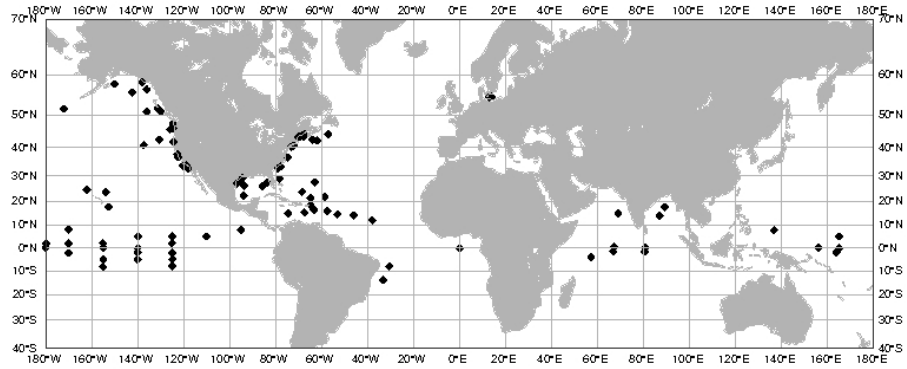

Figure 11: Locations of the moored buoys used in the comparisons.

	# of wind vectors	speed bias	stdev *u*	stdev *v*
25 km Metop-A	3957	0.11	1.52	1.78
25 km Metop-B	3799	0.03	1.56	1.73
25 km Metop-C	**3659**	**0.04**	**1.51**	**1.80**
12.5 km Metop-A	4975	0.11	1.62	1.95
12.5 km Metop-B	4761	0.10	1.62	1.90
12.5 km Metop-C	**4581**	**0.08**	**1.59**	**1.89**

Table 3: buoy comparison results of ASCAT 25 km and 12.5 km wind products from February to April 2019.

In Table 3 we show the wind speed bias and wind component standard deviations of the 25 km and 12.5 km wind products. It is clear that for each spatial resolution the statistics are very similar for Metop-A, Metop-B and Metop-C.

6. Triple collocation results

A triple collocation study was performed to initially assess the errors of the ASCAT, ECMWF, and buoy winds independently. The triple collocation method was introduced by Stoffelen [14]. Given a set of triplets of collocated measurements and assuming linear calibration, it is possible to simultaneously calculate the errors in the measurements and the relative calibration coefficients. The triple collocation method can give the measurement errors from the coarse resolution NWP model perspective, from the intermediate resolution scatterometer perspective, or from the fine resolution buoy perspective when using an estimated buoy observation error, mainly constituted by the spatial representativeness error of buoy data for a scatterometer WVC. How to deal with errors of spatial representation is extensively introduced by Vogelzang et al. [15].

Collocated data sets of ASCAT 25 km and 12.5 km, ECMWF and buoy winds spanning three months were used in the triple collocation. Table 4 lists the error variances of the buoy, ASCAT, and ECMWF winds from the intermediate resolution scatterometer perspective. When we compare the 12.5 km products with the 25 km products, we see not so much change in the buoy wind error standard deviations and an increase of the ECMWF wind standard deviations by approximately 0.1 m/s. The apparently larger ECMWF errors are due to the finer resolution of the 12.5 km product, which contains more small scale information and in this respect resembles worse the lower effective resolution ECMWF winds. The errors of the 12.5 km winds are larger than those of the 25 km winds. This is most probably due to the larger noise in the 12.5 km wind retrievals. The results for Metop-A, Metop-B, and Metop-C for each product resolution are comparable, the differences are due to the relative short period (3 months) used, giving only a limited collocation data set and hence somewhat larger uncertainties in the obtained error standard deviation numbers.

The scatterometer winds are of good quality: at 25 km scale the error in the wind components is less than 0.5 m/s; at 12.5 km scale it is less than 0.8 m/s.

	Scatterometer		Buoys		ECMWF	
	ε_u (m/s)	ε_v (m/s)	ε_u (m/s)	ε_v (m/s)	ε_u (m/s)	ε_v (m/s)
25 km Metop-A	0.41	0.52	1.17	1.29	1.27	1.33
25 km Metop-B	0.48	0.49	1.15	1.30	1.23	1.36
25 km Metop-C	**0.44**	**0.46**	**1.15**	**1.32**	**1.22**	**1.30**
12.5 km Metop-A	0.68	0.81	1.17	1.35	1.37	1.41
12.5 km Metop-B	0.62	0.78	1.18	1.31	1.36	1.46
12.5 km Metop-C	**0.67**	**0.78**	**1.18**	**1.34**	**1.40**	**1.39**

Table 4: Error standard deviations in u and v wind components from triple collocation of ASCAT 25 km and 12.5 km wind products with buoy and ECMWF forecast winds, seen from the scatterometer perspective. The results were obtained for the period of February to April 2019.

From the triple collocation analysis, we can also determine the calibration of the scatterometer winds. The calibration coefficients *a* and *b* relate the observed scatterometer wind *w* to the 'true' wind *t* according to $t = a \times w + b$. This is done separately for the *u* and *v* wind components. The results in Table 5 show

that the winds are well calibrated for all three instruments, with *b* values close to 0 and *a* coefficients close to 1.

	a_u	a_v	b_u (m/s)	b_v (m/s)
25 km Metop-A	0.978	0.974	0.029	-0.040
25 km Metop-B	0.983	0.992	-0.020	-0.025
25 km Metop-C	0.991	0.972	-0.024	-0.010
12.5 km Metop-A	0.987	0.965	-0.031	-0.079
12.5 km Metop-B	0.982	0.980	-0.063	-0.043
12.5 km Metop-C	0.993	0.964	-0.081	-0.068

Table 5: Calibration coefficients a and b for u and v wind components from triple collocation of ASCAT 25 km and 12.5 km wind products with buoy and ECMWF forecast winds. The results were obtained for the period of February to April 2019.

7. Comparison of EARS ASCAT winds with global winds

ASCAT winds are not only produced in the OSI SAF, but also in the EUMETSAT Advanced Retransmission Service (EARS), a network of ground stations receiving the Metop data directly and providing improved timeliness, typically 15 minutes between end of data acquisition and availability to the users. Although the EARS winds are produced outside the OSI SAF scope, we have included some validation results in this document since they are relevant to the wind users.

In order to assess the quality of the EARS wind products from Metop-C, the winds have been compared with the corresponding OSI SAF global wind products, which have already been validated in the previous sections of this report. The comparisons have been done by taking the global winds as a reference and finding the corresponding WVCs in the regional wind product. WVCs are considered to be collocated if they are not more than 17.7 km (25 km product) or 8.8 km (12.5 km product) apart (the WVC spacing divided by $\sqrt{2}$), and the acquisition times are within 30 minutes. The 30 minutes limit is to prevent mixing of data from different passes at high latitudes.

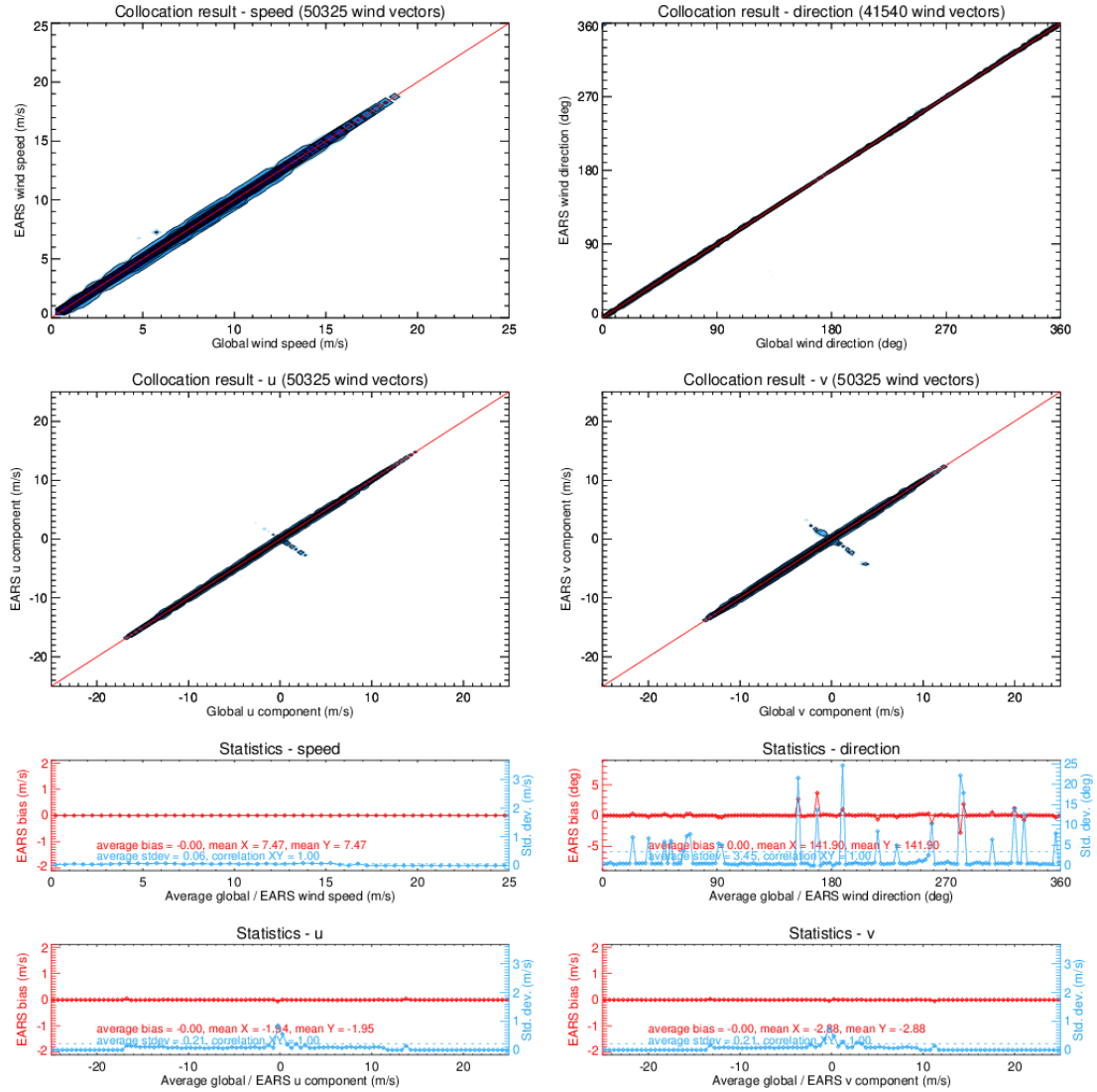

Figure 12: Comparison of 25 km ASCAT-C regional EARS wind product versus the global OSI SAF winds from 31 May 2019.

The global and EARS data flows are fully synchronised so the WVCs of global and regional data should be on the same location. This is because the same state vector information is used in the level0/1 processing of both global and regional data. However, in the coastal products the WVC locations can be displaced depending on the location of the full resolution data contributing to the average WVC backscatter. This may happen in particular near the beginning and ending of EARS regional passes where the number of full resolution observations used in the first or last row of WVCs may be lower. Note that if too few full resolution data are present, this will result in a high K_p (noise) value and the WVC will be rejected for wind inversion and hence no EARS wind will be computed.

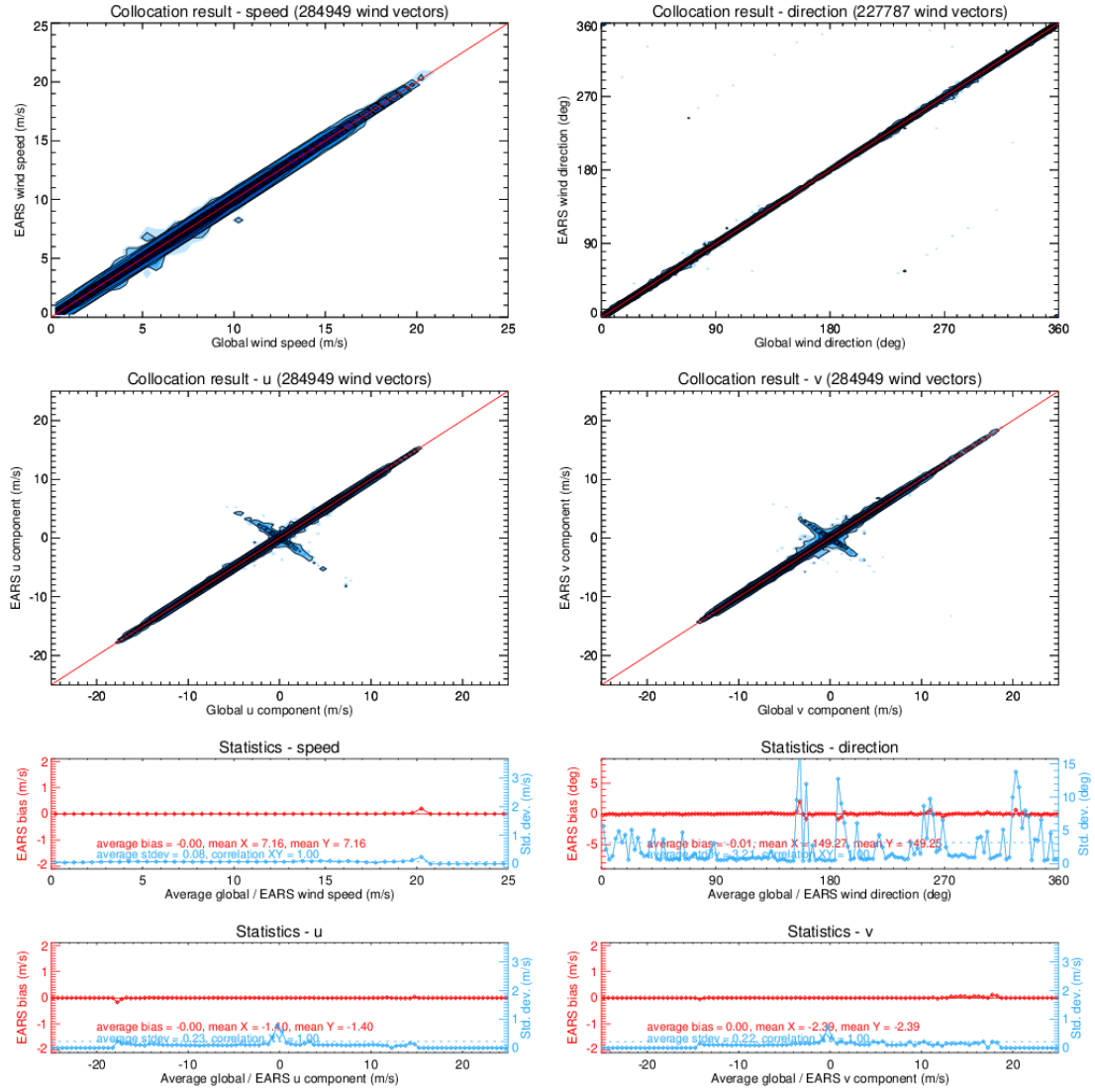

Figure 13: Comparison of 12.5 km ASCAT-C regional EARS wind product versus the global OSI SAF winds from 31 May 2019.

Figure 12 and Figure 13 show the collocation results of the ASCAT-C data from 31 May 2019. Most data are very close to the diagonals in the contour plots, but in the wind component plots there are clearly some side lobes representing differences in ambiguity selection in certain WVCs. This can be expected due to the granularity of the products which is different: the global data come in files containing 3 minutes of data, whereas the EARS data files contain a track of approximately 10 minutes in one file, the length

being determined by the time that the satellite is in the view of a ground station. Hence, the data batches that are fed into the ambiguity removal step are different and in few cases this leads to different wind selections, generally by 180 degrees or opposing vectors, particularly at low wind speeds. To further assess the influence of ambiguity removal in Figure 12 and Figure 13, we have repeated the statistics leaving out any WVCs with direction differences between EARS and global larger than 20 degrees. This effectively removes the side lobes in the plots (not shown). This filter removes 0.30% of the wind vectors at 25 km and 0.56% of the wind vectors at 12.5 km, i.e., only a small fraction of the ambiguity wind vector selection is affected by the product granularity.

We conclude that the regional EARS winds show a good correlation with the global OSI SAF winds. Wind differences are small and can be well explained by the ambiguity removal differences for both products which is connected with the product granularity.

8. Conclusions

Following established procedures, ASCAT-C backscatter corrections are derived with the use of NWP Ocean Calibration (NOC) to achieve improved backscatter value consistency and quality. These corrections are subsequently used in the ASCAT wind data processor (AWDP) where NOC corrections indeed show enhanced high quality, well calibrated winds. The NOC-calibrated ASCAT-C wind products are examined and their quality appears to be very similar to that of the ASCAT-A and ASCAT-B wind products. The characteristics of the 25 km product and the 12.5 km coastal product are very similar, but with more spatial detail in the higher resolution product, as expected.

The Metop-C ASCAT 25 km and 12.5 km wind products have been validated, mainly focussing on the comparison with the existing products from Metop-A and Metop-B. Looking at the global bulk statistics as obtained from comparisons with ECMWF model winds and buoy winds, the Metop-C products show similar characteristics as compared to the existing ones.

The products provide wind quality well within the OSI SAF product requirements [2]: better than 2 m/s in wind component standard deviation with a bias of less than 0.5 m/s in wind speed on a monthly basis. Regional EARS wind data have the same characteristics as the global OSI SAF wind data. ASCAT-C appears to be a successful successor of ASCAT-B and the user community may look forward to an interesting period of trifold ASCAT-A, ASCAT-B and ASCAT-C winds of high quality.

9. References

[1] OSI SAF,
Product Requirements Document,
SAF/OSI/CDOP3/MF/MGT/PL/2-001, 2018

[2] OSI SAF,
Service Specification Document,
SAF/OSI/CDOP3/MF/MGT/PL/003, 2018

[3] OSI SAF,
ASCAT Wind Product User Manual,
SAF/OSI/CDOP/KNMI/TEC/MA/126, 2019

[4] EUMETSAT,
ASCAT Level 1 Product Generation Function Specification
EUM.EPS.SYS.SPE.990009

[5] EUMETSAT,
ASCAT-C Level 1 Commissioning Report
EUM/RSP/REP/18/1035367, 2019

[6] Verspeek, J. A. Stoffelen, A. Verhoef and M. Portabella,
Improved ASCAT Wind Retrieval Using NWP Ocean Calibration
IEEE Transactions on Geoscience and Remote Sensing, 50, 2012, 2488-2494,
doi:10.1109/TGRS.2011.2180730

[7] Stoffelen, A.,
A Simple Method for Calibration of a Scatterometer over the Ocean
J. Atm. and Ocean Techn. 16(2), 1999, 275-282

[8] Stoffelen, A., J. Verspeek, J. Vogelzang and A. Verhoef,
The CMOD7 Geophysical Model Function for ASCAT and ERS Wind Retrievals,
IEEE Journal of Selected Topics in Applied Earth O, 2017, 10, 5, 2123-2134,
doi:10.1109/JSTARS.2017.2681806

[9] De Kloe, J., A. Stoffelen and A. Verhoef,
Improved Use of Scatterometer Measurements by using Stress-Equivalent Reference Winds,
IEEE Journal of Selected Topics in Applied Earth O, 2017, 10, 5, 2340-2347,
doi:10.1109/JSTARS.2017.2685242

[10] Stoffelen, A. and D. Anderson,
Scatterometer Data Interpretation: Measurement Space and inversion,
J. Atm. and Ocean Techn., 14(6), 1997, 1298-1313

[11] Belmonte Rivas, M., A. Stoffelen, J. Verspeek, A. Verhoef, X. Neyt and C. Anderson,
Cone Metrics: A New Tool for the Intercomparison of Scatterometer Records,
IEEE Journal of Selected Topics in Applied Earth O, 2017, 10, 5, 2195-2204,
doi:10.1109/JSTARS.2017.2647842

[12] Bidlot J., D. Holmes, P. Wittmann, R. Lalbeharry, and H. Chen
Intercomparison of the performance of operational ocean wave forecasting systems with buoy data
Wea. Forecasting, vol. 17, 287-310, 2002

[13] Liu, W.T., K.B. Katsaros, and J.A. Businger
Bulk parameterization of air-sea exchanges of heat and water vapor including the molecular constraints in the interface
J. Atmos. Sci., vol. 36, 1979

[14] Stoffelen, A.
Toward the true near-surface wind speed: error modeling and calibration using triple collocation
J. Geophys. Res. 103, C4, 7755-7766, 1998, doi:10.1029/97JC03180

[15] Vogelzang, J., A. Stoffelen, A. Verhoef and J. Figa-Saldana
On the quality of high-resolution scatterometer winds
J. Geophys. Res., 116, C10033, 2011, doi:10.1029/2010JC006640

10. Abbreviations and acronyms

ASCAT	Advanced Scatterometer
AWDP	ASCAT Wind Data Processor
EARS	EUMETSAT Advanced Retransmission Service
ECMWF	European Centre for Medium-Range Weather Forecasts
EUMETSAT	European Organisation for the Exploitation of Meteorological Satellites
GMF	Geophysical Model Function
GTS	Global Telecommunication System
KNMI	Royal Netherlands Meteorological Institute
LKB	Liu, Katsaros and Businger
Metop	Meteorological operational satellite
MLE	Maximum Likelihood Estimator
NASA	National Aeronautics and Space Administration
NOC	NWP-based Ocean Calibration
NWP	Numerical Weather Prediction
OC	Ocean Calibration
OSI	Ocean and Sea Ice
QC	Quality Control
SAF	Satellite Application Facility
u	West-to-east (zonal) wind component
v	South-to-north (meridional) wind component
WVC	Wind Vector Cell